

Decoupling Surface Analysis of  $\text{Cl}+\text{Cl}_2$  Reaction Embedded in  $\text{Ar}_{52}$  Cluster

Kiyohiko SOMEDA\* and Hiroki NAKAMURA

Division of Theoretical Studies, Institute for Molecular Science, Myodaiji, Okazaki 444

(Received April 21, 1994)

A model triatomic reaction  $\text{Cl}+\text{Cl}_2\rightarrow\text{Cl}_2+\text{Cl}$  embedded in an  $\text{Ar}_{52}$  van der Waals cluster is analyzed classically mechanically by a novel theoretical method called “decoupling surface analysis”. This method generates new reactive and vibrational variables in which the kinetic coupling as well as the potential coupling are minimized. An analysis of local frequencies of the vibrational variables along the reaction coordinate clarifies how the motions of ambient Ar atoms are coupled with the central  $\text{Cl}_3$  system. When the local frequencies are plotted as a function of the reaction coordinate, avoided crossings among these curves are observed. Mixing of Cl motion and Ar motion is clearly detected by these avoided crossings. The vibrational mode having a character of the symmetric stretch of  $\text{Cl}_3$  shows exclusively strong coupling with the reactive motion. This mode, however, very weakly couples with the ambient Ar motion. On the other hand, the bending and translation of  $\text{Cl}_3$  are strongly mixed with the motions of ambient Ar atoms and produce unstable modes, which play the most significant role in energy exchange between the central reaction system and the ambient Ar atoms.

To understand chemical reaction in solution is one of the ultimate goals of chemistry. Various approaches have long been made to this end;<sup>1–3)</sup> for example, the transition state theory,<sup>4)</sup> Kramers theory<sup>5,6)</sup> and Grote–Hynes theory have been pursued.<sup>7–9)</sup> These studies are more or less carried out from the macroscopic, i.e., the statistical mechanical, point of view. From the purely microscopic point of view, it is very significant to know how the reactive motions of reactants interact with the motions of ambient atoms and/or molecules. In this context many works based on molecular dynamics simulation have been carried out. For instance, the series of works done by Bergsma et al.<sup>10–12)</sup> brought a very clear global picture: Dynamics of the  $\text{Cl}+\text{Cl}_2\rightarrow\text{Cl}_2+\text{Cl}$  reaction in rare gas solution is almost the same as in gas phase, because the time scale of the reaction is much shorter than that of collision with ambient rare gas atoms;<sup>10,11)</sup> while in the case of  $\text{S}_\text{N}-2$  reaction in polar solvents the reaction is governed by the thermal motion of solvent molecules.<sup>12)</sup> The studies based on molecular dynamics simulation have thus served to grasp the gross features of reaction as a whole. Systematic analyses based on classical or quantum mechanics are, however, needed to clarify the reaction dynamics in more detail such as how the motions of the reactants interact with those of ambient atoms and/or molecules. It is indispensable for constructing a basic model of reaction in solution to know those solvent modes which are important for reaction by carrying out such microscopic dynamical analysis.

In the present study, classical mechanical analysis called decoupling surface analysis<sup>13)</sup> is employed. This is a kind of stability analysis of the vibrational motions which are chosen to be maximally decoupled from reactive motion. The analysis of local frequencies clarifies how the reactive motion is coupled to the motions of ambient atoms and molecules. In particular, the vibrational modes are classified into the following three types: unstable modes, strongly-coupled (stable)

modes, and weakly-coupled (stable) modes.

Since reaction takes place within a finite time interval and the effective spatial range of interaction in solvent is also finite, it suffices to consider finite number of ambient atoms (or molecules) surrounding the central reactant atoms. In the present study, the number of ambient atoms is truncated to be finite, and the intra-cluster reaction is considered.

As a central reaction system, we chose  $\text{Cl}+\text{Cl}_2\rightarrow\text{Cl}_2+\text{Cl}$  which Bergsma et al.<sup>10,11)</sup> devised as a generic model of chemical reaction. It should be noted, however, that the potential energy function Bergsma et al. assumed is not intended to actually mimic the real reaction of Cl. In the present study, the reaction  $\text{Cl}+\text{Cl}_2\rightarrow\text{Cl}_2+\text{Cl}$  is embedded in an Ar van der Waals cluster. The atomic radius of Ar is very close to that of Cl, and, therefore, Cl atoms can easily be included in the Ar clusters without drastic change of structure and stability of the clusters. It is known that the argon clusters  $\text{Ar}_n$  with  $n=13, 55, 147$  have icosahedral symmetry and are particularly stable.<sup>14)</sup> From these icosahedral clusters,  $\text{Ar}_{55}$  was chosen to be an ambience of the reaction system  $\text{Cl}+\text{Cl}_2\rightarrow\text{Cl}_2+\text{Cl}$ . Three central Ar atoms in  $\text{Ar}_{55}$  are replaced by Cl atoms to obtain  $\text{Cl}_3\text{Ar}_{52}$  reaction system.

Although effects of solvent on the electronic structure of the reactant atoms are of crucial significance especially when one discusses reaction in polar solvent, we focus our attention in the present study on the purely dynamical effects exerted by the nuclear motions of ambient Ar atoms under a given potential energy function. Such dynamical aspect is also one of the most intriguing features of reaction in solution.

The present paper is organized as follows. In Section I, the decoupling surface analysis is briefly surveyed in order to make this paper self-contained. The setup of the  $\text{Cl}+\text{Cl}_2\rightarrow\text{Cl}_2+\text{Cl}$  reaction in an Ar cluster is described in Section II. The results of the analysis is presented in Section III. Section IV summarizes the results

of the analysis.

### I. A Synopsis of the Decoupling Surface Analysis

Decoupling surface analysis<sup>13)</sup> is based on separation of reactive motion from vibrational motion transversal to it. By a variable transformation which mixes coordinates and momenta in the classical phase space, new reactive momentum and coordinate ( $\varepsilon, \tau$ ) and new vibrational momenta and coordinates ( $\mathbf{v}, \mathbf{u}$ ) are sought so that they are maximally decoupled from each other. The basic principle of decoupling is given by,

$$\left. \frac{\partial H}{\partial \mathbf{u}} \right|_{\mathbf{u}=\mathbf{v}=0} = \left. \frac{\partial H}{\partial \mathbf{v}} \right|_{\mathbf{u}=\mathbf{v}=0} = 0. \quad (1)$$

The two dimensional surface determined by  $\mathbf{u}=\mathbf{v}=0$  is called "decoupling surface", which is an extension of the conventional reaction path<sup>15-18)</sup> into the phase space. A mathematical consideration starting from Eq. 1 leads to the conclusion that the decoupling surface is a one-parameter family of classical trajectories, which we call "characteristic trajectories". Energy of the characteristic trajectories can be used as the new reactive momentum  $\varepsilon$ , and the reaction coordinate canonically conjugate to  $\varepsilon$  is time  $\tau$  along the characteristic trajectories. Boundary conditions of the decoupling surface, or of the characteristic trajectories, are imposed so that the new vibrational modes coincide with the conventional ones at a certain point in the configuration space. In the present study, the boundary condition is imposed at the saddle point of the potential energy surface of  $\text{Cl}_3\text{Ar}_{52}$ , i.e., at the saddle point the new vibrational modes are chosen to coincide with the vibrational modes perpendicular to the conventional reaction path. At other points the new vibrational modes differ from the conventional ones. In order to achieve the above boundary condition, the characteristic trajectories are shot from the saddle point in the direction tangential to the reaction path by changing the initial kinetic energy  $\varepsilon$ . The family of these characteristic trajectories with a parameter  $\varepsilon$  forms the decoupling surface.

The key quantity of the present analysis is a characteristic exponent  $\lambda$  of each vibrational mode obtained by solving the eigenvalue problem of the stability matrix defined at each point ( $\varepsilon, \tau$ ) on the decoupling surface. Details of the construction of the stability matrix is presented in Ref. 13. The eigenvalues of the stability matrix are called characteristic exponent  $\lambda$ , while the eigenvectors define the vibrational modes. Generally,  $\lambda$  is a complex number. When  $\lambda$  is pure imaginary, the corresponding vibrational mode is stable, and its (angular) frequency is given by  $\text{Im}\lambda$ . The action variable  $J$  of these stable modes are approximately conserved. If all the vibrational modes are stable, the time evolution of the reaction variables ( $\varepsilon, \tau$ ) is governed by the following effective Hamiltonian in one degree of freedom,

$$H_{\text{eff}}(\varepsilon, \tau) = \varepsilon + \sum_i J_i \text{Im}\lambda_i(\varepsilon, \tau), \quad (2)$$

where the subscript  $i$  labels vibrational mode. Details of  $H_{\text{eff}}$  can also be found in Ref. 13. Equation 2 implies that the stable vibrational modes exert their effects on the reactive degree of freedom through  $\varepsilon$ - and/or  $\tau$ -dependence of  $\lambda$ . As will be seen in section III, the stable modes can be classified under a certain qualitative criterion into a group having strong  $\tau$ -dependence and that having weak  $\tau$ -dependence. We name the former "strongly coupled (stable) mode" and the latter "weakly coupled (stable) mode". On the other hand, when  $\text{Re}\lambda \neq 0$  the corresponding mode is unstable. In the presence of unstable modes, the destination of a given trajectory sensitively depends on the vibrational phase angles of the unstable modes. In other words, the phase angles of the unstable modes decide whether a given trajectory is reactive or not. Thus the unstable modes exert decisive effects on the reactive motion.

### II. Construction of $\text{Cl}+\text{Cl}_2 \rightarrow \text{Cl}_2+\text{Cl}$ Reaction in $\text{Ar}_{52}$ Cluster

The present study intends to clarify the reactant-solvent interaction in view of reaction in solution. The central reaction system,  $\text{Cl}+\text{Cl}_2 \rightarrow \text{Cl}_2+\text{Cl}$ , is believed to have properties commonly possessed by many other chemical reactions.

Since time needed for reaction to complete is finite, the mutual influence between reactant and solvent can prevail over only a certain finite spatial range in solvent. Thus it suffices to consider a finite-size cluster of solvent atoms. As a solvent atom, Ar takes a special position, because its atomic radius is almost the same as that of Cl and Cl atoms can easily be embedded into Ar clusters without drastic change in their structure and stability. It is known that Ar van der Waals clusters of size  $n=13, 55, 147, 309, 561, \dots$  have icosahedral symmetry and particular stability in comparison with the other size of the clusters.<sup>14)</sup>  $\text{Ar}_{13}$  is composed of one central Ar atom and a single-fold surrounding shell. This is too small to be a model of solvent. On the other hand,  $\text{Ar}_{147}$  is too big from the practical point of view. Thus  $\text{Ar}_{55}$  is chosen in the present study as an ambience of the central reaction system.  $\text{Ar}_{55}$  is composed of one central atom and a two-fold surrounding shell and can be a good model of solvent.

In  $\text{Ar}_{55}$ , Ar atoms are located to form a regular icosahedron in the following manner:<sup>14)</sup> One "central atom" at the origin, twelve "vertex atoms" at the vertices of the icosahedron, twelve "inner edge atoms" at the middle points between the origin and the vertices, and thirty "outer edge atoms" at the middle points between the vertices. The three Ar atoms, i.e., the central atom and two inner edge atoms on the  $z$ -axis, are replaced by Cl atoms to obtain the  $\text{Cl}-\text{Cl}-\text{Cl}$  reaction system in  $\text{Ar}_{52}$  (see Fig. 1).

The potential energy function of the  $\text{Cl}-\text{Cl}-\text{Cl}$  system

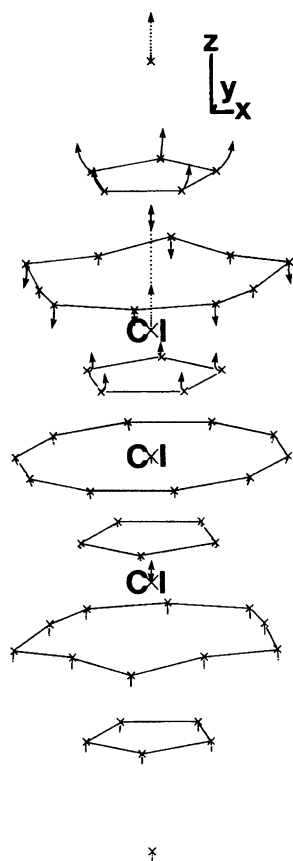


Fig. 1. Illustration of the structure at the saddle point of  $\text{Cl}_3\text{Ar}_{52}$  and the characteristic trajectory with  $\varepsilon = 0.01$  a.u. of the latter half reaction from the saddle point to the product. The scale of the  $z$ -axis is enlarged as indicated by the  $xyz$ -axes in the figure. On the small crosses Ar atoms are located, while the positions of Cl atoms are indicated by the large crosses. Dotted lines running from the crosses represent motions of Ar and Cl atoms along the characteristic trajectory with  $\varepsilon = 0.01$  a.u. The upper Cl atom is dissociating from the  $\text{Cl}_3$  and the Ar atoms surrounding it moves in accordance with the motion of the Cl atom.

is taken from that of Bergsma et al.<sup>10,11)</sup> It is the LEP type potential. It should be noted that this LEP potential is designed not to mimic the real chlorine atoms, but to be a generic model of chemical reaction. We call it "Cl atom" because the mass and the atomic radius corresponds to the real Cl. For Cl-Ar and Ar-Ar interaction, Lennard-Jones pairwise potential functions are adopted also by following Bergsma et al.<sup>10,11)</sup>

The saddle point of the reaction system is needed in the decoupling surface analysis as mentioned in the preceding section. This is obtained by the following procedure: (1) The size of the icosahedron formed by  $\text{Ar}_{55}$  is determined to minimize the total energy of  $\text{Ar}_{55}$ . (2) The three Ar atoms, i.e., the central atom and two inner edge atoms on the  $z$ -axis, are replaced by Cl, and the energy is minimized by taking icosahedral structure as an initial guess and by varying the positions of Ar

and Cl atoms under the condition that the two distances of neighboring Cl-Cl are kept equal to each other.

### III. Results of the Decoupling Surface Analysis

The structure of  $\text{Cl}_3\text{Ar}_{52}$  at the saddle point is displayed in Fig. 1. The characteristic trajectories were shot from the saddle point in the direction of antisymmetric stretch mode of  $\text{Cl}_3$ . The initial velocities of Ar atoms were set equal to zero. Due to the symmetry of the present reaction system, the decoupling surface analysis for the first half of the reaction, i.e., from the reactant to the saddle point, is the same as that for the latter half of the reaction, i.e., from the saddle point to the product. Thus it suffices to consider the latter half reaction.

A characteristic trajectory with its kinetic energy  $\varepsilon = 0.01$  a.u. is shown in Fig. 1. It can be seen that the motions of Ar atoms surrounding the recoiling Cl atom (the five Ar atoms on the uppermost pentagon in Fig. 1) and particularly the Ar atom subject to head-on collision with the Cl atom (the topmost Ar atom in Fig. 1) are included in the reactive degree of freedom. In that head-on collision, the kinetic energy of the recoiling Cl atom is transferred to the Ar atoms, and the dissipation of the energy begins. The characteristic trajectories depend on  $\varepsilon$  very weakly in the energy range  $0 < \varepsilon < 0.1$ . This is because the characteristic trajectories just go down-hill almost spontaneously, and their behavior is mainly determined by the topography of the potential. In other words, the initial kinetic energy at the saddle point has little effect on the behavior of trajectories in such a low energy range that is significant for discussing reaction in solution. It is thus suffice to examine the case of  $\varepsilon = 0.01$  a.u.

$\tau$ -Dependence of the characteristic exponents in the case of  $\varepsilon = 0.01$  a.u. is shown in Figs. 2, 3, and 4. At the right ends of Figs. 2, 3, and 4 the reaction is completed, while the left end corresponds to the saddle point. The huge peaks on the right ends of Figs. 2, 3, and 4 are not relevant to the reaction but to the dissipation of the released energy after the reaction is over. The left half part of Figs. 2, 3, and 4 is relevant to the reaction. The number of unstable modes depends on  $\tau$  as can be seen in Fig. 2. The three modes marked as  $\alpha$ ,  $\beta$ ,  $\gamma$  in Fig. 2 have major influence on the reaction. By examining the eigenvectors of the stability matrix at each  $\tau$ , we can "assign" their vibrational modes. At point A indicated in Fig. 2,  $\alpha$  mode is mainly composed of the linear combination of  $\text{Cl}_3$  antisymmetric stretch and  $\text{Cl}_3$  translation in the cluster. At point B,  $\beta$  mode has a character of the motion of the recoiling Cl atom in the  $x$ - $y$  plane. At point C,  $\gamma$  mode is the rotation of  $\text{Cl}_2$ . The other unstable modes having smaller  $\text{Re}\lambda$  are composed mainly of motions of Ar atoms.

Figure 3 displays  $\text{Im}\lambda$  along  $\tau$ . One mode, which we call  $a$  mode, has exclusively large frequency and  $\tau$ -dependence, and this mode can be classified into strongly-

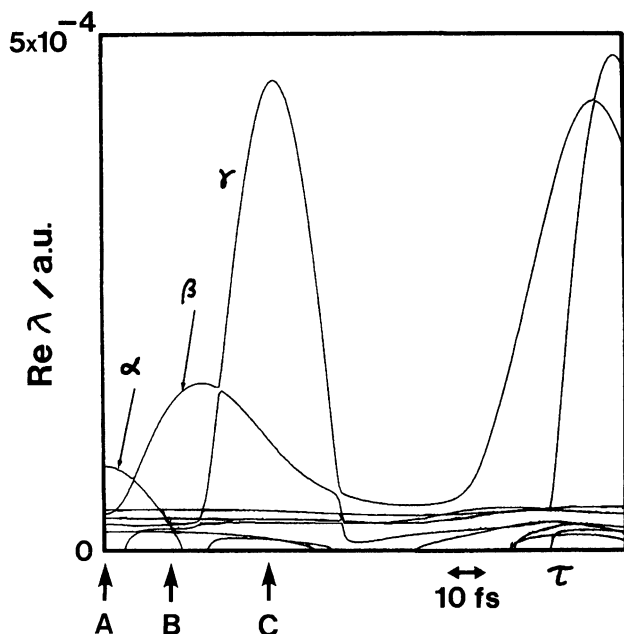


Fig. 2.  $\tau$ -Dependence of the real part of the characteristic exponent  $\lambda$ . The left end of the figure corresponds to the saddle point. At the right end of the figure the half reaction is completed. Point A corresponds to the saddle point, while at point C, the associating Cl-Cl distance achieves minimum during its oscillation.

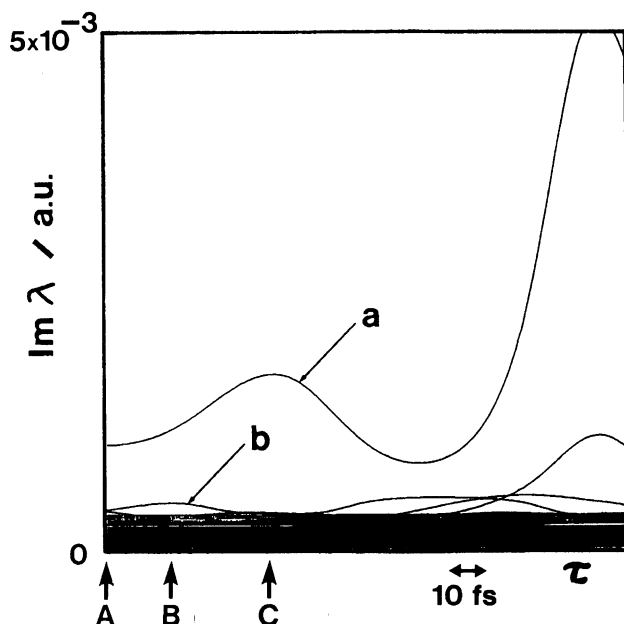


Fig. 3.  $\tau$ -Dependence of the imaginary part of the characteristic exponent  $\lambda$ . The left end of the figure corresponds to the saddle point. At the right end of the figure the half reaction is completed. Points A, B, and C are the same positions as in Fig. 2.

coupled (stable) mode. Inspection of the eigenvector shows that this mode is composed of the symmetric stretch of  $\text{Cl}_3$ , and that very little Ar motion is mixed

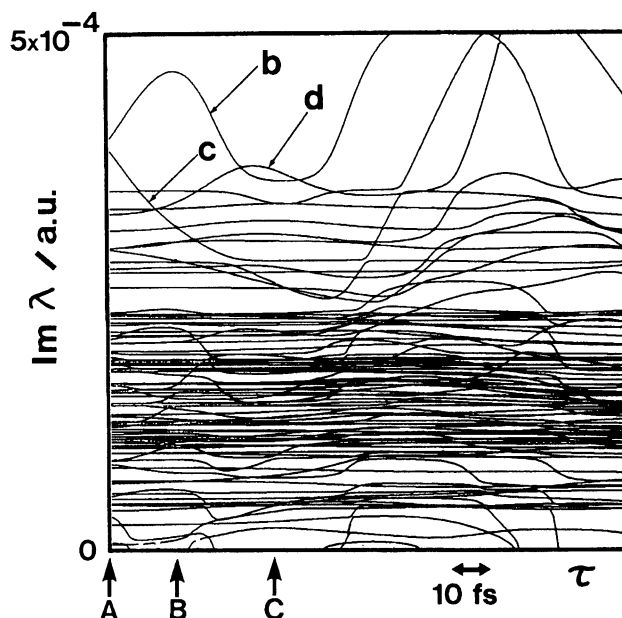


Fig. 4. A magnification of the small  $\text{Im } \lambda$  part of Fig. 3.

into it. This mode is the only vibrational mode same as that of  $\text{Cl} + \text{Cl}_2 \rightarrow \text{Cl}_2 + \text{Cl}$  in gas phase.

When one examines the low frequency part of Fig. 3, one finds more modes which have relatively strong  $\tau$ -dependence as can be seen in Fig. 4. The modes indicated by b, c, and d can be classified into strongly coupled modes, and they have characters similar to  $\gamma$ ,  $\beta$ , and  $\alpha$  modes, respectively. The other modes which have weaker  $\tau$ -dependence are composed of the motions of Ar atoms and classified into weakly coupled modes.

In Fig. 4, "avoided crossings" of the frequency curves are seen. This phenomenon has the same mathematical origin as that in the ordinary avoided crossings of adiabatic states, i.e., non-crossing of eigenvalues as a function of its parameter. As in the case of level crossings, the interchange of the character of eigenvectors is found to occur also in the present case. For example, b mode, which has the character of  $\text{Cl}_2$  rotation at point B as mentioned above, changes its character at point C, where it is composed of hindered rotations  $R_x$  and  $R_y$  of the two five-membered rings of Ar surrounding the associating Cl-Cl bond. At point C, c mode also has a different character from that at point A; it is out-of-plane deformation of the five-membered ring of Ar surrounding the recoiling Cl atom. Generally speaking, the flat modes in Figs. 2, 3, and 4 have a main character of Ar motion, while the oscillatory modes in these figures are of  $\text{Cl}_3$  motion. It should also be noted that when the frequency curve of b mode in Fig. 4 descends to cause an avoided crossing with horizontal frequency curves of Ar modes, the unstable  $\gamma$  mode rises in Fig. 2. The similar phenomenon occurs in the pair of d and  $\alpha$  modes. When the d mode is flat, the  $\alpha$  mode has a hump, and vice versa. The pair of c and  $\beta$  modes seems also to be in such relation, although it is not so

evident as in the cases of  $b$ - $\gamma$  and  $d$ - $\alpha$  pairs. The characters of the unstable and strongly coupled modes and the correlation among them are summarized in Fig. 5.

The following picture based on the avoided crossings is useful to understand how the motions of  $\text{Cl}_3$  interact with the motions of ambient Ar atoms: The Cl motions have strong  $\tau$ -dependence, simply because they are directly connected to the central reaction. On the other hand, the Ar motions have much lower frequencies than those of  $\text{Cl}_3$  due to the softness of the van der Waals cluster, and their frequencies have very weak  $\tau$ -dependence. The symmetric stretch of  $\text{Cl}_3$ , which is perpendicular to the reactive variables, has much higher frequency than that of Ar motion, and accordingly, does not mix with Ar motion. Thus the symmetric stretch of  $\text{Cl}_3$  becomes  $a$  mode by itself. Due to this independence from Ar motion, the behavior of  $a$  mode is almost the same as that of the corresponding reaction in gas phase. On the other hand, bending of  $\text{Cl}_3$  at the saddle point correlates with rotation of  $\text{Cl}_2$  in the product region, i.e., it becomes zero-frequency mode in gas phase. Accordingly, when embedded in the Ar cluster, the frequency of this bending mode decreases with  $\tau$ , and consequently, its frequency curve crosses with that of an Ar mode to cause avoided crossing. This avoided crossing induces mixing between Cl motion and Ar motion. The bending mode, which is doubly degenerate in gas phase, is the origin of  $b$  and  $c$  modes, and their characters are transferred to unstable  $\gamma$  and  $\beta$  modes, respectively, through the avoided crossings. As regards the pair of  $d$  and  $\alpha$  modes, it correlates with the translation of  $\text{Cl}_2$  in the  $z$  direction in gas phase. It is also zero-frequency mode in gas phase and becomes *vibrational* mode when embedded in the cluster. Its frequency is very sensitive to the size of  $\text{Cl}_3$ , and consequently, has strong  $\tau$ -dependence. Thus this mode is also subject to avoided

crossing with Ar modes and produce unstable  $\alpha$  mode and strongly coupled (stable)  $d$  mode. These character-transfers cause energy transfer between the reactants and the solvent atoms since the reactant modes at the saddle point become the solvent modes in the course of reaction, and vice versa.

#### IV. Conclusion

The decoupling surface analysis was applied to the reaction  $\text{Cl} + \text{Cl}_2 \rightarrow \text{Cl}_2 + \text{Cl}$  embedded in an Ar van der Waals cluster. The local vibrational modes are analyzed along the reaction coordinate  $\tau$  defined in the decoupling surface analysis, and particularly, the  $\tau$ -dependence of the frequencies and characters of the vibrational modes is examined. The vibrational modes can be classified into the following three types: (1) unstable mode, (2) strongly coupled (stable) mode, and (3) weakly coupled (stable) mode. The avoided crossings among the frequency vs.  $\tau$  curves give a clue to understand the interaction between the central reaction and the motions of the ambient Ar atoms. The picture obtained from the present analysis is summarized as follows: Basically, all the modes of  $\text{Cl}_3$  strongly depend on  $\tau$ , simply because they are directly involved in the reaction. On the other hand, the modes of the solvent motion have much lower frequencies than the  $\text{Cl}_3$  modes, and their frequencies depend on  $\tau$  very weakly even when the  $\text{Cl}_3$  reaction system is introduced into the cluster. The symmetric stretch of  $\text{Cl}_3$  in gas phase has much higher frequency than those of Ar clusters, and consequently, it does not mix with the solvent motion even when the reaction system is embedded in the cluster. Although this mode is strongly coupled with the reactive motion through strong  $\tau$ -dependence of its frequency, it hardly interacts with the solvent motion during the reaction process. The bending of  $\text{Cl}_3$  becomes zero-frequency mode when  $\text{Cl}-\text{Cl}_2$  bond breaks. When embedded in the cluster, the frequencies of the modes originating from the bending of  $\text{Cl}_3$  decrease with  $\tau$ , and inevitably, their frequency curve encounters the avoided crossing with the curves of Ar modes to cause mixing of the  $\text{Cl}_3$  bending and the solvent motion. Translation of  $\text{Cl}_3$  is also zero-frequency mode in gas phase, and therefore, subject to the avoided crossings with the solvent motion when embedded in the cluster. These avoided crossings produce dynamical coupling between the reactive motion and the ambient Ar motions.

The present work was supported in part by a Grant-in-Aid for Scientific Research on Priority Area "Theory of Chemical Reactions" from the Ministry of Education, Science and Culture. The numerical computations were carried out at the computer center of the Institute for Molecular Science.

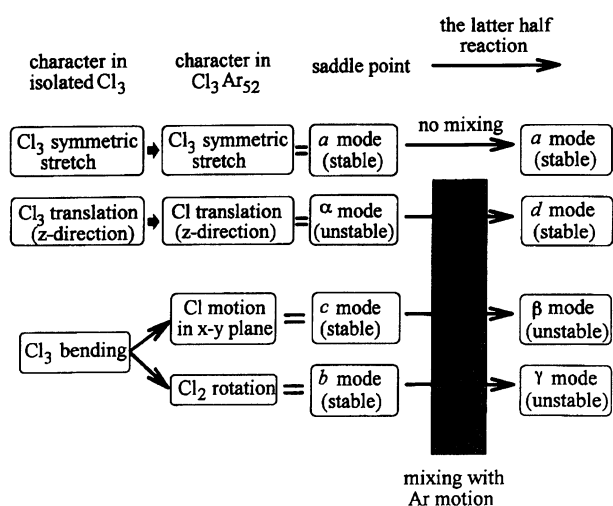


Fig. 5. A schematic diagram summarizing the characters of the vibrational modes, the correlation among them, and their changes in the course of the latter half reaction.

## References

- 1) B. Berne, M. Borkovec, and J. E. Straub, *J. Phys. Chem.*, **92**, 3711 (1988).
  - 2) J. N. Onuchic and P. G. Wolynes, *J. Phys. Chem.*, **92**, 6495 (1988).
  - 3) K. R. Wilson and R. D. Levine, *Chem. Phys. Lett.*, **152**, 435 (1988).
  - 4) H. Eyring, *J. Chem. Phys.*, **3**, 107 (1935).
  - 5) H. A. Kramers, *Physica (Utrecht)*, **7**, 284 (1940).
  - 6) P. Hanggi, P. Talkner, and M. Borkovec, *Rev. Mod. Phys.*, **62**, 251 (1990).
  - 7) R. F. Grote and J. T. Hynes, *J. Chem. Phys.*, **73**, 2715 (1980).
  - 8) R. F. Grote and J. T. Hynes, *J. Chem. Phys.*, **75**, 2191 (1981).
  - 9) R. F. Grote and J. T. Hynes, *J. Chem. Phys.*, **77**, 3736 (1982).
  - 10) J. P. Bergsma, P. M. Edelsten, B. J. Gertner, K. R. Huber, J. R. Reimers, K. R. Wilson, S. M. Wu, and J. T. Hynes, *Chem. Phys. Lett.*, **123**, 394 (1986).
  - 11) J. P. Bergsma, J. R. Reimers, K. R. Wilson, and J. T. Hynes, *J. Chem. Phys.*, **85**, 5625 (1986).
  - 12) J. P. Bergsma, B. J. Gertner, K. R. Wilson, and J. T. Hynes, *J. Chem. Phys.*, **86**, 1356 (1987).
  - 13) K. Someda and H. Nakamura, *J. Chem. Phys.*, **94**, 4260 (1991).
  - 14) M. R. Hoare, *Adv. Chem. Phys.*, **40**, 49 (1979).
  - 15) R. A. Marcus, *J. Chem. Phys.*, **45**, 4493 (1966).
  - 16) K. Fukui, S. Kato, and H. Fujimoto, *J. Am. Chem. Soc.*, **97**, 1 (1975).
  - 17) W. H. Miller, N. C. Handy, and J. E. Adams, *J. Chem. Phys.*, **72**, 99 (1980).
  - 18) W. H. Miller, *J. Phys. Chem.*, **87**, 3811 (1983).
-